Direct Field Orientation Control Based on H_∞ Method of Wind Turbine Based on DFIG

Bakou Youcef *[1,2], Saihi Lakhdar[2], Abid Mohamed[1], Hammaoui Youcef[2]

[1]IRECOM Laboratory (Interaction Réseaux Electriques Convertisseurs Machines),
Djillali Liabes University of Sidi Bel-Abbes, Algeria,
[2] Unité de Recherche en Energies Renouvelables en Milieu Saharien URERMS,
Centre de Développement des Energies Renouvelables CDER, 01000, Adrar, Algeria,
*Corresponding author; Email: youcefbakou@gmail.com

Article Info

Article history:

Received May 15, 2022
Revised June 09, 2022
Accepted June 13, 2022

Keywords:

Wind energy
DFIG
Direct field orientation control
H-infinity method
PI controller

ABSTRACT

This study aims to propose the direct field orientation control based on the H-infinity method (DFOC_ H_∞) scheme for controlling the stator power (active/ reactive) of a direct drive vertical axis wind turbine power system based on a doubly fed induction generator (DFIG). the sensitivity to parameters uncertainty of the machine presents the major drawback of the *PI* controller, in order to cope with this problem; the H-infinity method was used to solve it. The proposed controller H_∞ is evaluated with Matlab/Simulink. Simulation results showed that the suggested H_∞ controller has a good performance in terms of enhancing the quality of energy provided to the power network. Even in the presence of DFIG parameter variation.

I. Introduction

Wind energy is one of the most frequently applied methods of power generation among the many different types of renewable energy resources because of its financial benefits and compatibility with power grids in many locations[1]. To improve the performance of wind power generation, researchers from the industrial and academic sectors have recently devoted their efforts to it[2]–[4].
To ensure national energy security and diversify domestic energy sources, Algeria has an ambitious plan to develop renewable energy as a solution[5]. Large variations from one location to another define Algeria's wind resource. On average, speeds more than 3 m/s are present on 78 % of Algeria's surface, with roughly 40 % of these speeds reaching 5 m/s. Speeds in the South are higher than in the North (more than 6 m/s), which is advantageous for the use of wind energy in hybrid or wind farm plants[3], [6], [7].
Indeed, due to its numerous benefits, including their lower size and the ability to manage their active/reactive power through their rotor side converter, doubly fed induction generators (DFIG) are currently the most popular type generator used on wind turbines system[8], [9]. There have been numerous DFIG controllers researched and developed[10]. Due to its benefits of simple structure and good steady-state performance, the stator flux vector control based on proportional-integral (PI) controller is widely used in industrial applications; however, PI controller is based on the need to understand machine parameters. The main weakness of the PI controller is that the machine is sensitive to parameter uncertainty[11], [12]. The H-infinity approach was utilized to solve this problem.

II. Wind Energy Conversion System Model

The goal of the wind energy system is to transform the kinetic energy of the wind into electrical energy. This is done by a mechanism made up of a wind turbine, a generator, and a control section that oversees the entire system[13].

III.1 Wind Turbine Model

H-rotor wind turbine is used in this works, in a vertical axis wind turbine system, three blades are usually fixed to a vertical shaft rotor, which turns a generator to convert wind energy into electricity[14]. The model of the power rotor is given by:

$$P_{aro} = \frac{1}{2} C_p \rho R h V^3 \tag{1}$$

Where; C_p is the power coefficient, ρ is the air density (1.225 kg/m3), R is turbine rotor radius and h the turbine height, V is the wind speed (m/s).

The aerodynamic torque can be written as follows:

$$T_{aer} = \frac{P_{ae}}{\Omega_t} = \frac{C_p \rho R h V^3}{2\Omega_t} \tag{2}$$

with; Ω_t is the turbine speed (tr/min) and λ is the tip speed ratio can be written as follows:

$$\lambda = \frac{R\Omega_t}{V} \tag{3}$$

III.2 DFIG Model

The following equations provide the dynamic voltages and fluxes in *dq* reference frame that can be written using the Park model of the DFIG[15].

$$\begin{cases} v_{ds} = R_s i_{ds} + \frac{d\varphi_{ds}}{dt} - \omega_s \varphi_{qs} \\ v_{qs} = R_s i_{qs} + \frac{d\varphi_{qs}}{dt} + \omega_s \varphi_{ds} \\ v_{dr} = R_r i_{dr} + \frac{d\varphi_{dr}}{dt} - (\omega_s - \omega_r)\, \varphi_{qr} \\ v_{qr} = R_r i_{qr} + \frac{d\varphi_{qr}}{dt} - (\omega_s - \omega_r)\, \varphi_{dr} \end{cases} \tag{4}$$

Where; $i_{ds}, i_{qs}, \varphi_{ds}, \varphi_{qs}$ are the direct and quadrature components stator current, flux respectively, R_s is the stator resistance, ω_s is the synchronous angular speed. $i_{dr}, i_{qr}, \varphi_{dr}, \varphi_{qr}$ are the direct and quadrature components rotor current, flux respectively, R_r is the rotor resistance, ω_r is the rotational speed.
Stator and rotor flux:

$$\begin{cases} \varphi_{ds} = l_s i_{ds} + l_m i_{dr} \\ \varphi_{qs} = l_s i_{qs} + l_m i_{qr} \\ \varphi_{dr} = l_r i_{dr} + l_m i_{ds} \\ \varphi_{qr} = l_r i_{qr} + l_m i_{qs} \end{cases} \tag{5}$$

The electromagnetic torque is expressed by[16]:

$$T_{em} = p\frac{3L_m}{2L_s}(\varphi_{qs} i_{dr} - \varphi_{ds} i_{qs}) \quad (6)$$

Where, p is the number of pole pairs.
The mechanical expression is done as[9], [17]:

$$T_g - T_{em} = J\frac{d\Omega_t}{dt} + f\Omega_t \quad (7)$$

The stator powers are defined as[13]:

$$\begin{cases} P_s = v_{ds} i_{ds} + v_{qs} i_{qs} \\ Q_s = v_{qs} i_{ds} - v_{ds} i_{qs} \end{cases} \quad (8)$$

III. Vector Control Based on H∞ Method

One of the most used methods for managing electrical machines is vector control. It is founded on the machine's semblance to a DC machine with distinct excitation, the latter of which guarantees a natural decoupling between currents and flux[18]. In this works we used the direct field orientation control (DFOC). This technique involves ignoring the coupling terms and using a H∞ controller to manage the active and reactive power separately for each axis.
by applying an orientation on the *d* axis

$$\varphi_{ds} = \varphi_s, \varphi_{qs} = \frac{d\varphi_{qs}}{dt} = 0 \quad (9)$$

On the other hand, in steady state, it is assumed that the flow is constant[19], [20], thus:

$$\begin{cases} \boldsymbol{v_{ds} = 0} \\ \boldsymbol{v_{qs} = v_s = \omega_s \varphi_s} \end{cases} \quad (10)$$

According to FOC, the expressionof the electromagnetic torque and stator powers active and reactive are simplified as [21], [22]:

$$\begin{cases} T_{em} = -p\frac{3L_m}{2L_s}(\varphi_s \frac{l_m}{l_s} i_{qr}) \\ P_s = -v_s \frac{l_m}{l_s} i_{qr} \\ Q_s = -v_s \frac{l_m}{l_s} i_{dr} + \frac{{v_s}^2}{l_s.\omega_s} \end{cases} \quad (11)$$

By regulating the rotor currents of the DFIG, the stator powers (active and reactive) of the DFIG are controlled. To prove this, a relationship between the rotor currents and rotor voltages is shown[18]:

$$\begin{cases} v_{dr} = R_r i_{dr} + l_r \sigma \frac{di_{dr}}{dt} - (g\omega_s l_r \sigma i_{qr}) \\ v_{qr} = R_r i_{qr} + l_r \sigma \frac{di_{qr}}{dt} + g\omega_s l_r \sigma i_{dr} + g\frac{l_m v_s}{l_s} \end{cases} \quad (12)$$

with; $\sigma = (1 - \frac{{l_m}^2}{l_s.l_r})$

IV.1 H_∞Control Design

The robust H_∞ control problem has received a lot of attention lately. It is a crucial solution for system uncertainty and instability. Designing highly reliable controllers for both active and reactive power based on H_∞ method is the goal of this study. Determining the controller function $K(s)$ that minimizes the H_∞ norm of the transfer function while internally stabilizing the controlled dynamics closed-loop is the major challenge of the H∞ control technique[23].
The H_∞ synthesis employs the conventional problem concept, which is depicted in Figure 1[2]. The dynamic interactions between two sets of inputs and two sets of outputs are modeled by the $G(s)$ transfer matrix, which are augmented with weighting transfer function $W_n(s)$: The external inputs, such as noise, disturbances, and reference signals, are represented by the vector $\boldsymbol{w}$; The vector u represents the commands; the $\boldsymbol{e}$ signals are selected to represent the correct functioning of system; and $\boldsymbol{y}$ represents the measures available to develop the order.

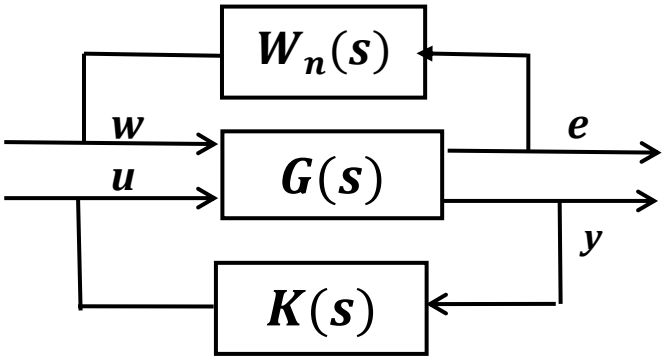

Figure 1. H_∞ synthesis design of typical problem

The relationship between input and output defined as[9], [24]:

$$\left\| \begin{matrix} W_1(s)S(s) & W_1(s)W_3(s)S(s)G(s) \\ W_2(s)K(s)S(s) & W_2(s)K(s)W_3(s)S(s)G(s) \end{matrix} \right\|_\infty < \gamma \tag{13}$$

Where; γ is a specified positive number, in this case equal one.
Numerous characteristic transfer matrices are produced as a result of the interaction between inputs and outputs. such as:
$S(s)$ is the sensitivity function defined as:

$$S(s) = \frac{1}{1+K(s)G(s)} \tag{14}$$

$T(s)$ is the complementary sensitivity function defined as:

$$T(s) = \frac{1}{G(s)K(s)(1+G(s)K(s))} \tag{15}$$

To find the controller $K(s)$, should be satisfies the following condition[2]:

$$\left\| \begin{matrix} W_1 S \\ W_2 KS \\ W_3 T \end{matrix} \right\|_\infty < \gamma \tag{16}$$

Where; $W_1$and W_3 are selected as follow[2], [25] :

$$w_1(s) = \frac{1+T_2 s}{\gamma(1+T_1 s)} \tag{17}$$

$$w_3(s) = \frac{1+T_3 s}{(1+T_4 s)} \tag{18}$$

Where; ω_c is the cut-off frequency of the system $G(s)$,$T_1=1/\omega_1$,$T_2=1/\omega_2$,$T_3=1/\omega_3$ and $T_4=1/\omega_4$. ($\omega_1 < \omega_2 < \omega_c$) and ($\omega_c < \omega_3 < \omega_4$).

IV. Simulation Results and Discussions

The wind energy conversion system's (WECS) nominal parameters are shown in Table 1. Figure 2 shows the simulation model diagram developed for this work. The presented DFOC-based H_∞ controller of the wind energy conversion system is tested for performance and stability using simulations performed using SIMULINK in the MATLAB software. The frequency dependent weighting function is described below. the design of w_1 was selected in order to shape the sensitivity function for enhanced disturbance rejection and minimal tracking error. The design of w_3 aimed to adjust the behavior of the complementary sensitivity function $T(s)$ in low and medium frequencies. Note that the KS and T have the same function[2], it is sufficient to fixed w_2 as a constant.

$w_1(s) = \frac{0.13S+660}{750S+1}$, $w_2(s) = 1$ and $w_3(s) = \frac{9s+100}{12S+25\ 10^3}$

The final controller $K_\infty(s)$ is given as:

$$K_\infty(s) = \frac{3.09\ 10^5 s^2 + 6.75\ 10^7 s + 3.757\ 10^9}{s^3 + 7.05\ 10^9 s^2 + 5.072\ 10^{11} s + 6.879\ 10^{13}}$$

Table 1. Nominal parameters of WECS

Power coefficient C_p	0.29
Number of blades	3
Radius of wind turbine R	4.45 m
Turbine height h	7.4 m
Air density $\boldsymbol{\rho}$	1.225 kg m^{-3}
Moment of total inertia J	35 Kg m^2
Tip speed ratio λ	2.5
Nominal power	15 kW
Stator frequency f	50 Hz
Viscous friction f_r	0.02 Nm
Stator resistance R_s	1.317 Ω
Rotor resistance R_r	1.037 Ω
Stator inductance L_s	0.0945 H
Rotor inductance L_r	0.0540 H
Mutual inductance L_m	0.0596 H

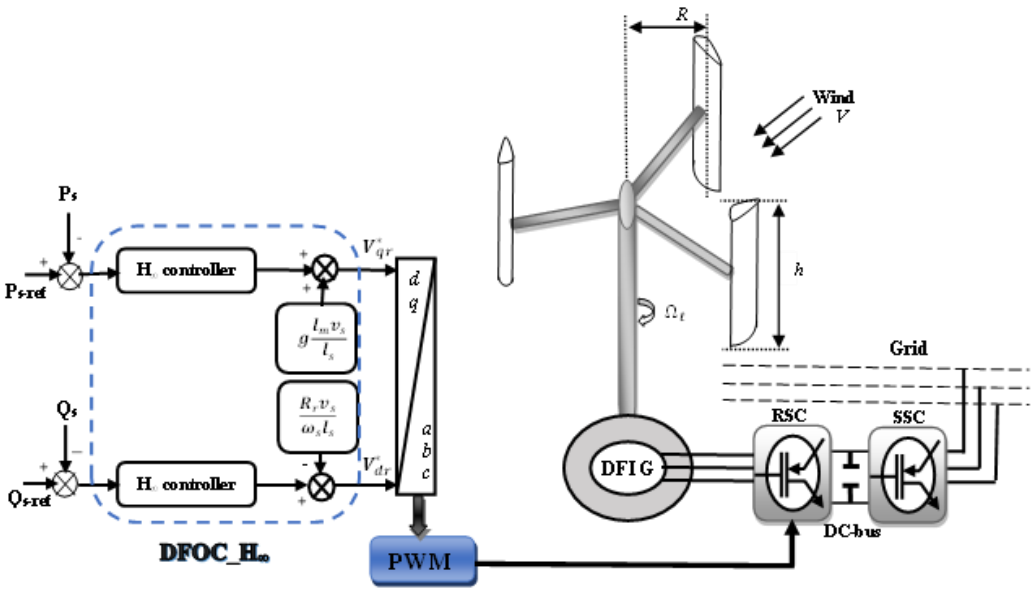

Figure 2. Control structure of the WECS based on DFIG with DFOC_H∞

Figure 3 presents the sensitivity function $S(s)$ and its bound $\gamma/w_1(s)$, complementary sensitivity functions $T(s)$ and its bound $\gamma/w_3(s)$. It is very clear; the infinity norm of the equation (14) is satisfied.

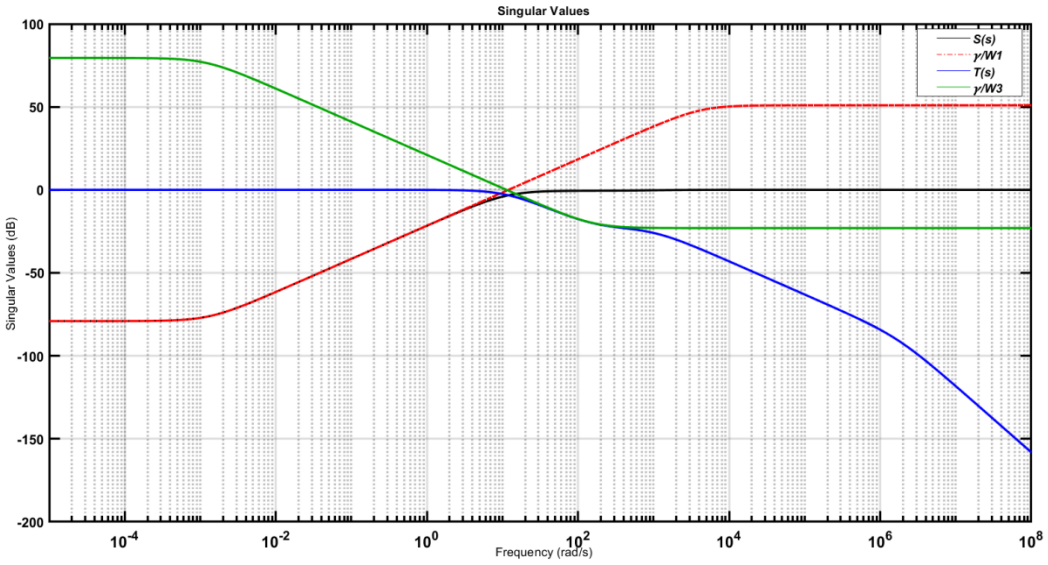

Figure 3. Frequency response of sensitivities, Complementary sensitivity and weightings functions.

Figure 4 is presented wind speed applied on turbine on (m/s) , Fig. 5 and Fig. 6 presents the stator active and reactive powers respectively of DFIG controlled by the proposed DFOC_H∞ (red line), *PI* (blue line), and their references(black line).

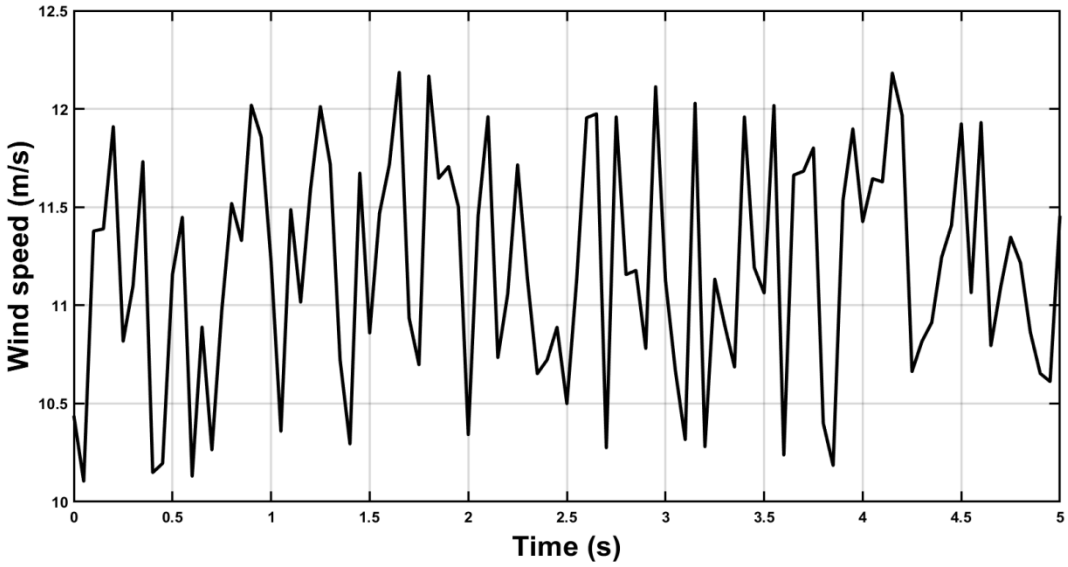

Figure 4. Wind speed profile

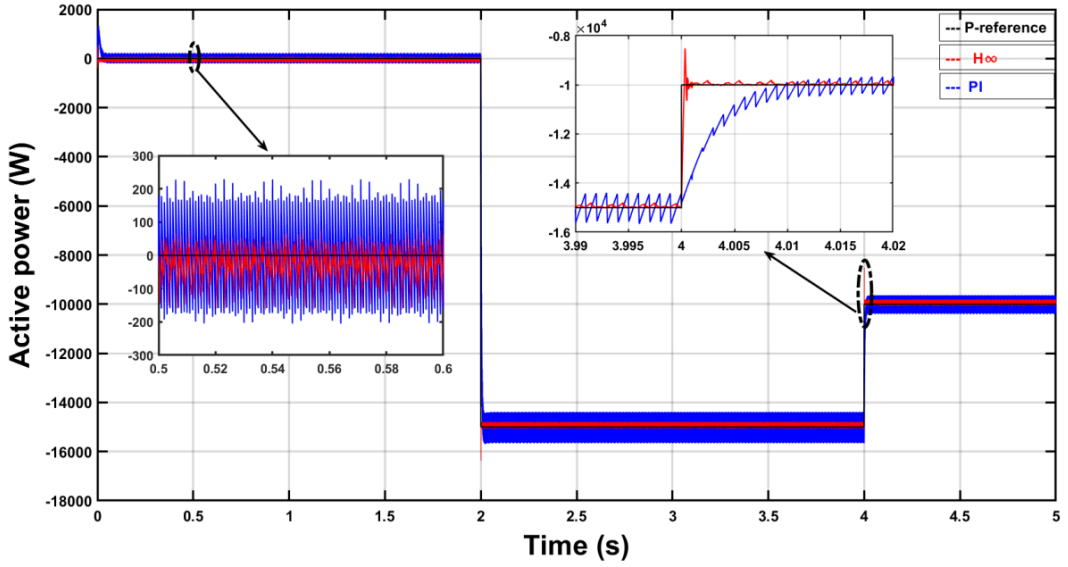

Figure 5. Active power of DFIG with DFOC_H$_\infty$ and PI controller

The results show that the strong decoupling between the stator active power and reactive power is maintained, and all of the controllers are effectively tracking their reference with major advantages of H_∞ controller in term error static, is a very low.

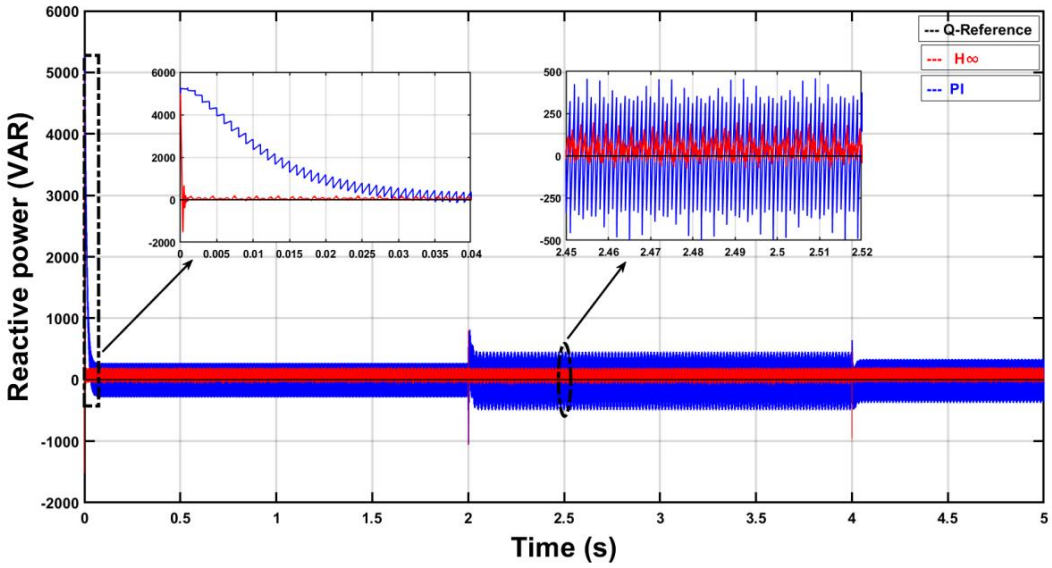

Figure 6. Reactive power of DFIG with DFOC_H_∞ and PI controller

Furthermore, using FFT (Fast Fourier Transform) approach, the total harmonic distortions (THD) of stator currents are presented in Figure 7 and Figure 8, as shown, The H_∞ controller reduce THD down to 2.91 % (Figure 8), compared to *PI* controller where THD is 12.81 % (Figure 7). The stator current signal quality of H_∞ controller has a good sinusoidal shape and less corrugate compared to *PI* controllers that leads to improving the quality of energy supply to grid is batter.

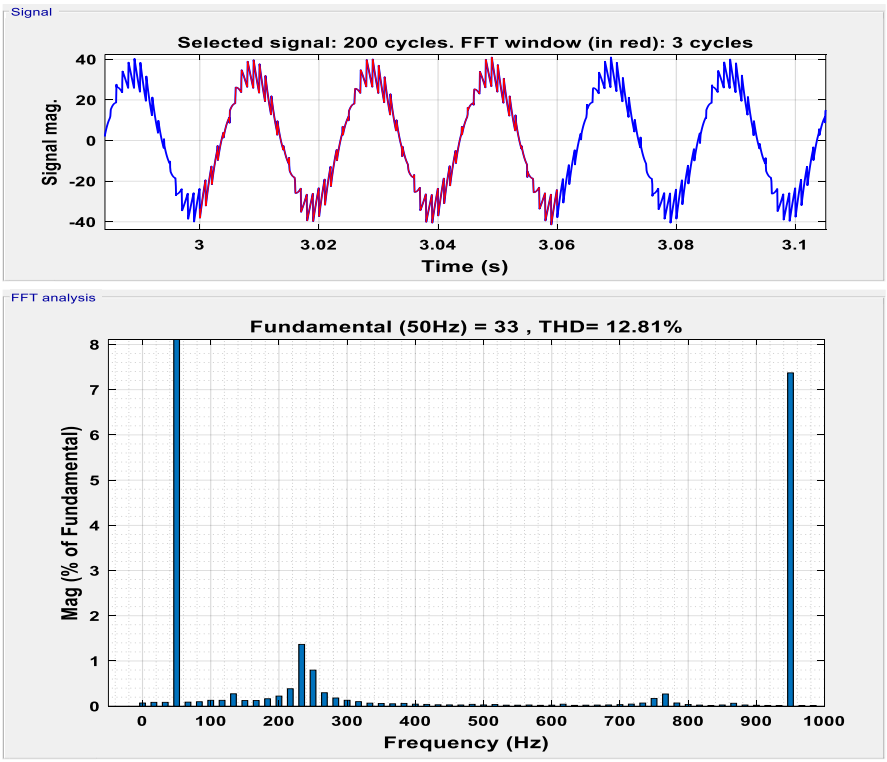

Figure 7. Stator currents THD with *PI* controller

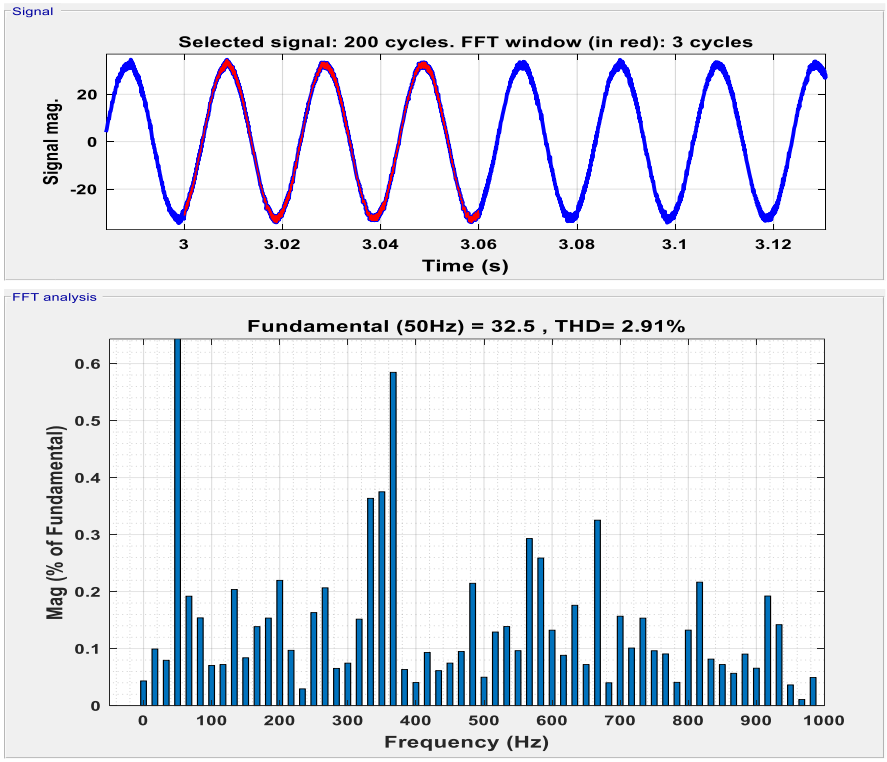

Figure 8. Stator currents THD with H_∞ controller

IV.1 Robustness Test

In order to compare the proposed controller's robustness to PI controllers, this test aims to examine and evaluate the effects of parametric changes on the H_∞ controller. The inductances L_s, L_r and L_m of DFIG ,reduced by 30% of its nominal value.

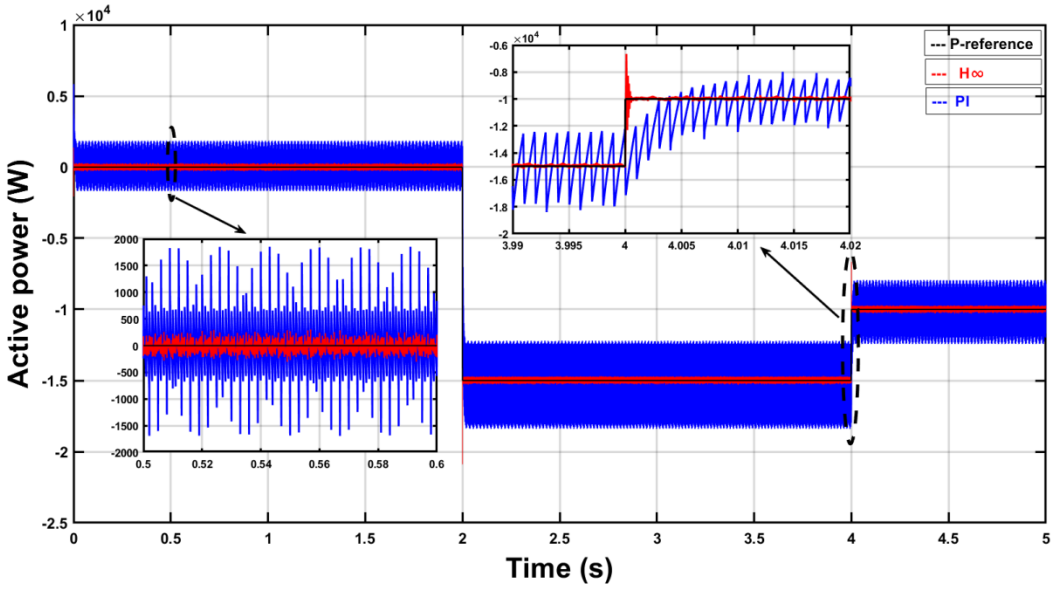

Figure 9. Impact of inductances variation L_s, L_r and L_m on stator active power

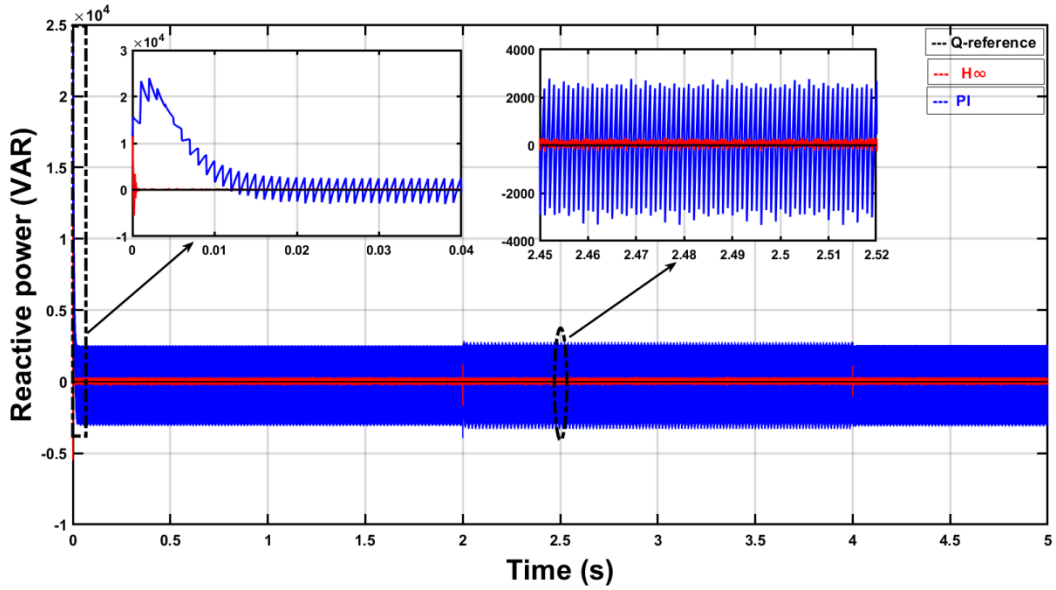

Figure 10. Impact of inductances variation L_s, L_r and L_m on stator reactive power

Figure 9 and 10 shows that the suggested controller has no effect on active and reactive power levels when inductance varies, whereas the PI controller has a large increase in corrugation at the level of active and reactive power, which affects the network's power quality supply.

V. Conclusion

The direct field orientation control based on H-infinity approach (DFOC_H_∞) of vertical axis wind turbine system associated with DFIG connected directly to the grid by the stator has been presented in this study. The results of simulation obtained with the proposed control (DFOC_H_∞) compared to the conventional *PI*, it can be concluded that this technique (DFOC_H_∞) is more efficient in tracking a time-varying trajectory, robustness face to the machine parameters variation, and the control axes were decoupled to a high degree. This helps DFIG-based devices like wind energy conversion systems guarantee very reliable electricity generation.

References

[1] L. Saihi *et al.*, "Hybrid control based on sliding mode fuzzy of DFIG power associated WECS," *AIP Conf. Proc.*, vol. 2123, no. July, 2019, doi: 10.1063/1.5117046.

[2] Y. Bakou *et al.*, "Design of Robust Control Based on R∞ Approach of DFIG for Wind Energy System," *Proc. - 2019 IEEE 1st Glob. Power, Energy Commun. Conf. GPECOM 2019*, pp. 337–341, 2019, doi: 10.1109/GPECOM.2019.8778584.

[3] A. Harrouz, A. Temmam, and M. Abbes, "Renewable Energy in Algeria and Energy Management Systems," *Int. J. Smart grid*, vol. 2, no. 1, 2017, doi: 10.20508/ijsmartgrid.v2i1.10.g9.

[4] A. Tayebi, M. Brahami, M. Yaichi, and A. Boutadara, "Low complexity SVM technique of control implementation by microcontroller for three phase solar inverter," *Environ. Prog. Sustain. Energy*, vol. 38, no. 6, pp. 1–10, 2019, doi: 10.1002/ep.13271.

[5] A. Tayebi, M. Brahami, M. Yaichi, and B. Abdelkader, "Design and Implementation of SVM for Three Phase Inverter Fed an Induction Motor for Photovoltaic Stand-alone Pumping System," in *2019 7th International Renewable and Sustainable Energy Conference (IRSEC)*, Nov. 2019, no. June, pp. 1–6. doi: 10.1109/IRSEC48032.2019.9078208.

[6] R. ABBAS, A. Harrouz, D. Belatrache, and V. DUMBRAVA, "Simulation and Optimization of a Wind Energy System in the Adrar Region," *Alger. J. Renew. Energy Sustain. Dev.*, vol. 3, no. 2, pp. 198–215, Dec. 2021, doi: 10.46657/ajresd.2021.3.2.9.

[7] A. Bouraiou *et al.*, "Status of renewable energy potential and utilization in Algeria," *J. Clean. Prod.*, vol. 246, 2020, doi: 10.1016/j.jclepro.2019.119011.

[8] S. Liang, Q. Hu, and W. J. Lee, "A survey of harmonic emissions of a commercially operated wind farm," *IEEE Trans. Ind. Appl.*, vol. 48, no. 3, pp. 1115–1123, 2012, doi: 10.1109/TIA.2012.2190702.

[9] L. Saihi, B. Berbaoui, H. Glaoui, L. Djilali, and S. Abdeldjalil, "Robust sliding mode H∞ controller of DFIG based on variable speed wind energy conversion system," *Period. Polytech. Electr. Eng. Comput. Sci.*, vol. 64, no. 1, pp. 53–63, 2020, doi: 10.3311/PPee.14490.

[10] Y. Bakou *et al.*, "DTC Control of the DFIG, Application to the Production of Electrical Energy," in *2019 8th International Conference on Renewable Energy Research and Applications (ICRERA)*, Nov. 2019, vol. 5, pp. 910–915. doi: 10.1109/ICRERA47325.2019.8996947.

[11] H. Chojaa, A. Derouich, S. E. Chehaidia, O. Zamzoum, M. Taoussi, and H. Elouatouat, "Integral sliding mode control for DFIG based WECS with MPPT based on artificial neural network under a real wind profile," *Energy Reports*, vol. 7, pp. 4809–4824, 2021, doi: 10.1016/j.egyr.2021.07.066.

[12] A. Sobhy and D. Lei, "Model-assisted active disturbance rejection controller for maximum efficiency schemes of DFIG-based wind turbines," *Int. Trans. Electr. Energy Syst.*, vol. 31, no. 11, pp. 1–21, 2021, doi: 10.1002/2050-7038.13107.

[13] I. Yaichi, A. Semmah, P. Wira, and S. M. El-Amine, "An improved Direct Power Control based on SVM strategy of the Doubly Fed Induction Generator," *Proc. 2019 7th Int. Renew. Sustain. Energy Conf. IRSEC 2019*, 2019, doi: 10.1109/IRSEC48032.2019.9078163.

[14] K. Roummani *et al.*, "A new concept in direct-driven vertical axis wind energy conversion system under real wind speed with robust stator power control," *Renew. Energy*, vol. 143, pp. 478–487, 2019, doi: 10.1016/j.renene.2019.04.156.

[15] Y. Bakou *et al.*, "Robust Controller Based on Sliding Mode Technique of DFIG Integrated to Wind Energy System," *2019 7th Int. Conf. Smart Grid*, pp. 144–148, Dec. 2019, doi: 10.1109/icSmartGrid48354.2019.8990687.

[16] L. Saihi and R. Gwsl, "Fuzzy-Sliding Mode Control Second Order of Wind Turbine Based on DFIG," pp. 6–10, 2022.

[17] L. Saihi, "Robust Sensor-less SMC under Variable-Speed Wind Turbine Systems of DFIG based on FKE," no. 4, pp. 301–305, 2022.

[18] M. Allam, M. Allam, and Y. Djeriri, "Etude comparative entre la commande vectorielle directe et indirecte de la Machine Asynchrone à Double Alimentation (MADA) dédiée à une application éolienne," *J. Adv. Res. Sci. Technol.*, vol. 1, no. 2, pp. 88–100, 2014.

[19] A. Bouyekni, R. Taleb, Z. Boudjema, and H. Kahal, "O RIGINAL SCIENTIFIC PAPER A second-order continuous sliding mode based on DPC for wind-turbine-driven DFIG," vol. 85, no. January, pp. 29–36, 2018.

[20] I. Yaichi *et al.*, "An improved DTC strategy for a DFIG using an artificial neural network controller," *9th Int. Conf. Smart Grid, icSmartGrid 2021*, pp. 231–237, 2021, doi: 10.1109/icSmartGrid52357.2021.9551251.

[21] I. Yaichi, A. Semmah, M. Djlaila, A. Harrouz, S. Mansouri, and Y. Bakou, "Modelling and control of doubly fed induction machine, application for a wind turbine system," *Proc. 2016 Int. Renew. Sustain. Energy Conf. IRSEC 2016*, pp. 450–455, 2017, doi: 10.1109/IRSEC.2016.7983953.

[22] J. Mohammadi, S. Vaez-Zadeh, S. Afsharnia, and E. Daryabeigi, "A combined vector and direct power control for DFIG-based wind turbines," *IEEE Trans. Sustain. Energy*, vol. 5, no. 3, pp. 767–775, 2014, doi: 10.1109/TSTE.2014.2301675.

[23] Y. Wang, Q. Wu, R. Yang, G. Tao, and Z. Liu, "Electrical Power and Energy Systems H ∞ current damping control of DFIG based wind farm for sub-synchronous control interaction mitigation," *Electr. Power Energy Syst.*, vol. 98, no. November 2017, pp. 509–519, 2018, doi: 10.1016/j.ijepes.2017.12.003.

[24] L. V. Assiene Mouodo, J. G. Tamba, O. S. Mayi, and L. Bibaya, "H-Infinity Control of an Adaptive Hybrid Active Power Filter for Power Quality Compensation," *Energy Power Eng.*, vol. 12, no. 11, pp. 603–640, 2020, doi: 10.4236/epe.2020.1211037.

[25] B. E. Sedhom, A. Y. Hatata, M. M. El-Saadawi, and E. H. E. Abd-Raboh, "Robust adaptive H-infinity based controller for islanded microgrid supplying non-linear and unbalanced loads," *IET Smart Grid*, vol. 2, no. 3, pp. 420–435, 2019, doi: 10.1049/iet-stg.2019.0024.